DNS Study on the Drag Reducing Flow with Additives Employing Giesekus Fluid Model and MINMOD Scheme - Effect of Weissenberg Number on the Turbulent Flow Structure -

Bo Yu[1,2], Yasuo Kawaguchi[1], Shu Takagi[3] and Yoichiro Matsumoto[3]
1. Turbomachinery Research Group, Institute for Energy Utilization, National Institute of Advanced Industrial Science and Technology, 1-2 Namiki, Tsukuba, Ibaraki 305-8564, Japan
2. Center for Smart Control of Turbulence
3. Dept. Mech. Eng. The University of Tokyo

ABSTRACT
In this article, a second order finite difference scheme was employed for the DNS study of the drag-reducing Giesekus fluid flow in a two-dimensional channel. A second-order bounded scheme, MINMOD, was used to discretize the convective term in the constitutive equation. The instantaneous stress and flow structures at different Weissenberg numbers are compared. Effects of Weissenberg number on various turbulence statistics such as turbulence intensities, Reynolds shear stress and two-point correlation coefficients are also presented.

INTRODUCTION
It is well known that a small amount of chemicals such as water-soluble polymers or surfactants cause dramatic suppression of turbulence when they are added to the liquid flow at large Reynolds numbers (Toms, 1948). In recent two-decades, the application of surfactant to the heat transportation system such as district heating/cooling system is attracting the interest of researchers. It has been revealed that 70% of pumping power to drive the hot water in primary pipeline of district heating system was saved by adding only few hundred ppm of surfactant into the circulating water.
This technological achievement requires a new designing strategy for pipe line network, fittings and heat exchangers to handle the drag reducing liquid flow. For the case of Newtonian fluid such as water or air, the knowledge to design fluid system is well accumulated and the accuracy of numerical prediction is sufficient. In the other hand, the designing method of viscoelastic fluid system is far from satisfaction. For example, the friction factor of specific solution in the straight pipe becomes not only a function of Reynolds number but also the pipe diameter. We cannot predict how much drag reduction will be achieved when it flows in straight tube from liquid sample.
The authors are making the investigation of the drag reduction by additives using the experimental and numerical approach. The final target is offering the designing strategy of viscoelastic fluid system at high Reynolds number and find the controlling method of turbulence suppression. This research may also possible to offer some common understanding for the turbulence suppression/enhancement and drag reduction/increase mechanism realized by variety of methods such as wall modification, particle suspension, bubble mixture or individual eddy control. Experimental study to clarify the turbulent structure and heat transfer mechanism and to find the termination method of turbulent suppression in heat exchanger are now undergoing. In this article, the part of numerical study is presented.

Recently some direct numerical simulations have been performed to investigate the basic mechanism of additive-induced drag-reduction flow. Orlandi (1995) and DenToonder et al. (1997) employed elongational viscosity models to study the turbulent drag-reduction channel flow and pipe flow, respectively. Sureshkumar et al.(1997) and Dimitropoulos et al. (1998) used viscoelastic models (FENE-P model and Giesekus model). In order to prevent

numerical breakdown, artificial terms were added into the constitutive equations (Sureshkumar et al.(1997) and Dimitropoulos et al. (1998)). An onset criterion, $12.5 < We_\tau < 25$, was proposed by Sureshkumar et al. (1997) and Dimitropoulos et al. (1998) based on the numerical solutions. Min et al. (2001) obtained a smaller onset Weissenberg number by using a high-order compact difference scheme with local artificial diffusion term in the constitutive equation. The present authors, for the first time, used a high-resolution scheme, MINMOD, for the viscoelastic turbulent flow (Yu et al. (2002)). It is found that by using the MINMOD scheme, the calculation procedure becomes more stable and the results have more spatial resolution than those by the artificial diffusion method.

The authors have been performing experimental analysis on drag-reducing flow by additives (Li et al.(2001)) and rheological properties of the solution. We find the Giesekus model can qualitatively describe our measured apparent shear viscosity and extensional viscosity. Based on the experimental results, properties of the surfactant solution do not confrict to those of a Giesekus fluid. Our final aim is to use the model parameters obtained from the experiments to simulate our experimental drag-reducing flow, and now the exact parameters are in the analyzing procedure. In this article all the model parameters are set artificially. The purpose of the present study is to numerically study the effect of Weissenberg number on the drag-reducing Giesekus fluid flow.

GOVERNING EQUATIONS AND NUMERICAL METHOD

We simulated the drag-reducing flow in a 2D channel. The flow geometry and the coordinate are shown in Figure 1, in which *x*, *y* and *z* are the streamwise, normal and spanwise direction respectively. The height of the channel is $2h$.

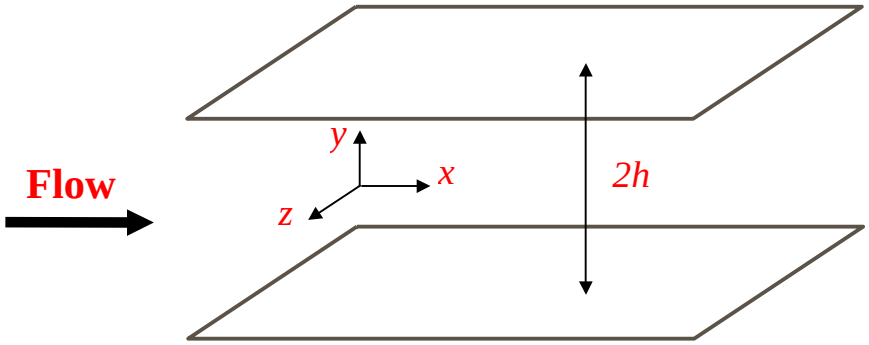

Figure 1: Coordinate system in channel

The fluid is assumed incompressible, isothermal with constant properties. The dimensionless governing equations for the unsteady incompressible Giesekus fluid are as follows:

Continuity equation:

$$\frac{\partial u_i^+}{\partial x_i^+} = 0 \tag{1}$$

Momentum equation:

$$\frac{\partial u_i^+}{\partial t^*} + u_j^+ \frac{\partial u_i^+}{\partial x_j^*} = -\frac{\partial p^+}{\partial x_i^*} + \frac{\beta}{\mathrm{Re}_\tau} \frac{\partial}{\partial x_j^*}\left(\frac{\partial u_i^+}{\partial x_j^*}\right) + \frac{1-\beta}{We_\tau} \frac{\partial c_{ij}^+}{\partial x_j^*} \tag{2}$$

Constitutive equation:

$$c_{ij}^{+}-\delta_{ij}+\alpha\left(c_{im}^{+}-\delta_{im}\right)\left(c_{mj}^{+}-\delta_{mj}\right)+\frac{We_{\tau}}{\mathrm{Re}_{\tau}}\left(\frac{\partial c_{ij}^{+}}{\partial t^{*}}+\frac{\partial u_{m}^{+}c_{ij}^{+}}{\partial x_{m}^{*}}-\frac{\partial u_{i}^{+}}{\partial x_{m}^{*}}c_{mj}^{+}-\frac{\partial u_{j}^{+}}{\partial x_{m}^{*}}c_{mi}^{+}\right)=0 \tag{3}$$

where t^{*} is the time, p^{+} the hydrostatic pressure, u_{i}^{+} the velocity component and c_{ij}^{+} the conformation stress. $(\,)^{*}$ is normalized by h and $(\,)^{+}$ is normalized by u_{τ},μ and ρ. The parameter β is the ratio of solvent contribution to the total zero-shear viscosity. The Reynolds number and Weissenberg number are defined as: $\mathrm{Re}_{\tau}=\rho u_{\tau}h/\mu$ and $\mathrm{We}_{\tau}=\rho\lambda u_{\tau}^{2}/\mu$, where ρ, μ, λ, u_{τ} and h are the fluid density, the solvent contribution to the viscosity, the relaxation time, the friction velocity and half of the channel height respectively. Our computations are carried out for $\mathrm{Re}_{\tau}=150$, $\beta=0.9$ and four Weissenberg numbers: $\mathrm{We}_{\tau}=2,\ 12.5,\ 30$ and 45.

The periodic boundary conditions are imposed in both the streamwise and spanwise direction, while nonslip condition is adopted for the top and bottom walls. The computational domain size is $L_{x}\times L_{y}\times L_{z}=10h\times 2h\times 5h$. Uniform grids are used in the streamwise and spanwise directions. Nonuniform grids are used in the normal direction with denser mesh near the wall to resolve small eddies. A transformation is used as follows:

$$y_{j}=\frac{h}{a}\tanh\left(\frac{1}{2}\zeta_{j}\ln\frac{1+a}{1-a}\right) \tag{4}$$

with

$$\zeta_{j}=-1+2\frac{j}{N_{2}} \tag{5}$$

where a is an adjustable parameter of the transformation and N_{2} is gird number in the normal direction. A constant value of $a=0.95$ is adopted herein. Figure 2 compares the mean velocity profile and turbulence intensities by using two sets of grids: $64\times64\times64$ and $64\times128\times64$ grids (in the *x*-,*y*- and *z*- direction respectively). It can be seen that the results for the two sets of grids agree well with each other. To save computational time, the $64\times64\times64$ grids are used in the present study.

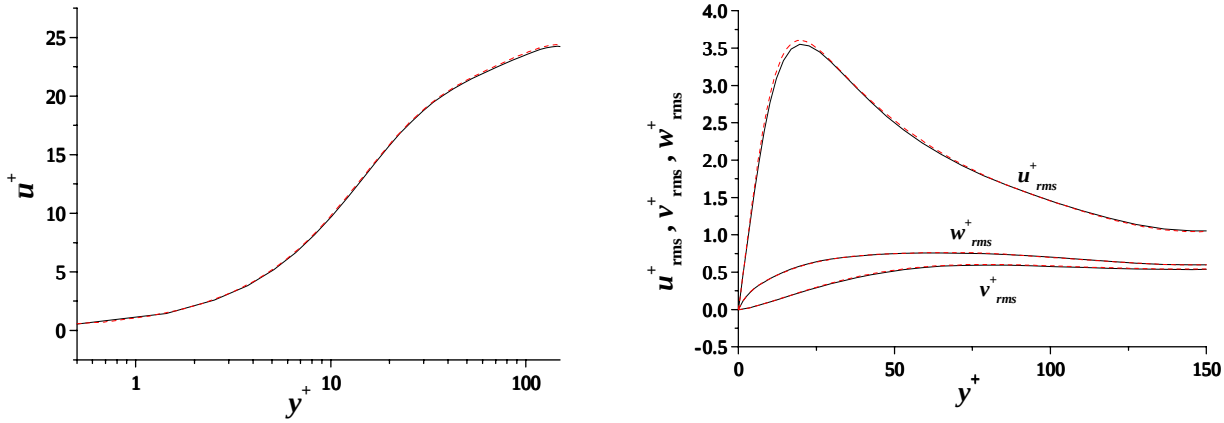

Figure 2: Left: The mean velocity profile and Right: Root mean square velocity fluctuations for $\beta=0.9,\mathrm{Re}_{\tau}=150,\mathrm{We}_{\tau}=30$ and $\alpha=0.001$ with two different grids: $64\times64\times64$ grids (black solid line) and $64\times128\times64$ grids(red dash line).

Numerical simulations of viscoelastic flow are prone to break down at high Weissenberg number due to the hyperbolic nature of the constitutive equations. To overcome this trouble,

artificial diffusion spectral method (Sureshkumar et al.(1997) and Dimitropoulos et al. (1998)) and local artificial diffusion finite difference scheme (Min et al. (2001)) were employed. We compared the performance of artificial diffusion scheme with a high-resolution scheme, MINMOD, for the 2D drag-reducing flow (Yu et al.(2002)). It was found that MINMOD scheme is much more stable and has higher spatial resolution than the artificial diffusion method. In this study, the MINMOD scheme is used to discretize the convective term in the constitutive equations.

The staggered grids are used to prevent zigzag pressure field. For time integration, Adams-Bashforth scheme is used for all the terms except that implicit method is used for the pressure term. The MAC method is used to couple velocity and pressure.

RESULTS AND DISCUSSION

Figure 3 compares the statistical steady values for $\beta = 0.9$, $\mathrm{Re}_\tau = 150$ and four Weissenberg numbers $\mathrm{We}_\tau = 2, 12.5, 30$ and 45. For comparison, the case for Newtonian fluid, i.e., $\beta = 1.0$ is also presented. The streamwise mean velocity profiles are shown in Figure 3 (a). It is seen at $\mathrm{We}_\tau = 2$, the nondimensionalized velocity profile is slightly smaller than that of Newtonian case. This means not any drag-reduction occurs and a slightly drag- enhancement. For $\mathrm{We}_\tau = 12.5, 30$ and 45, the velocity profiles are up shifted at the buffer and logarithmic layers as compared to that of the Newtonian case. The larger flow rates means drag-reductions occur. In this study, we define the drag-reduction rate as the decrease percentage of the friction factor as compared to Newtonian fluid flow at the same mean flow Reynolds number base on the height of the channel, $\mathrm{Re}_m = 2\rho u_m h / \mu = 2\,\mathrm{Re}_\tau\, u_m^+$. The calculated mean Reynolds numbers and the corresponding friction factors are shown in Table 1. We did not do the calculations for the Newtonian cases for those mean Reynolds numbers. But we can estimate the friction factors at those Reynolds numbers by using the experimental correlation $f = 0.073(\mathrm{Re}_m)^{-0.25}$ (Dean, 1978). Then the drag-reduction rates are obtained and listed in Table 1. Apparently the drag-reduction rate at $\mathrm{We}_\tau = 12.5$ is appreciable. We did calculation for the case $We_\tau = 8$, not appreciable drag reduction was observed. Thus using MINMOD scheme, the onset Weissenberg number obtained in the present study is around 10. Note that not any appreciable drag-reduction is obtained at $\mathrm{We}_\tau = 12.5$ by artificial diffusion spectral method (Sureshkumar et al.(1997) and Dimitropoulos et al. (1998)). A higher onset Weissenberg number $12.5 < We_\tau < 25$ was predicted. This indicates the artificail diffusion term deterioates the solution accuracy. Moreover it is clear from Figure 3(a) that the larger the Weissenberg number, the larger the buffer layer becomes.

Table 1
Mean Reynolds Numbers, Friction Factors and Drag-Reduction Rate

Weissenberg number	12.5	30	45
Mean Reynolds number	4838	6180	6936
Friction factor	0.00769	0.00471	0.00374
Drag-reduction rate	12.1%	42.8%	53.2%

Figure 3 (b)-(d) compares the root mean square velocity fluctuations. It can be seen that the for the smallest Weissenberg number $\mathrm{We}_\tau = 2$, the turbulence intensities are almost the same as those of Newtonian results. With the increase of Weissenberg number, the root mean square velocity fluctuations in the streamwise direction are enhanced. The larger the Weissenberg number is, the larger the u^+_{rms} becomes. As compared to Newtonian results, the location of the maximum u^+_{rms} shifts toward the centerline of the channel for drag-reduction cases. The larger the drag-reduction rate, the further the location shifts to the bulk flow. This is corresponding to an increased buffer layer with the increase of

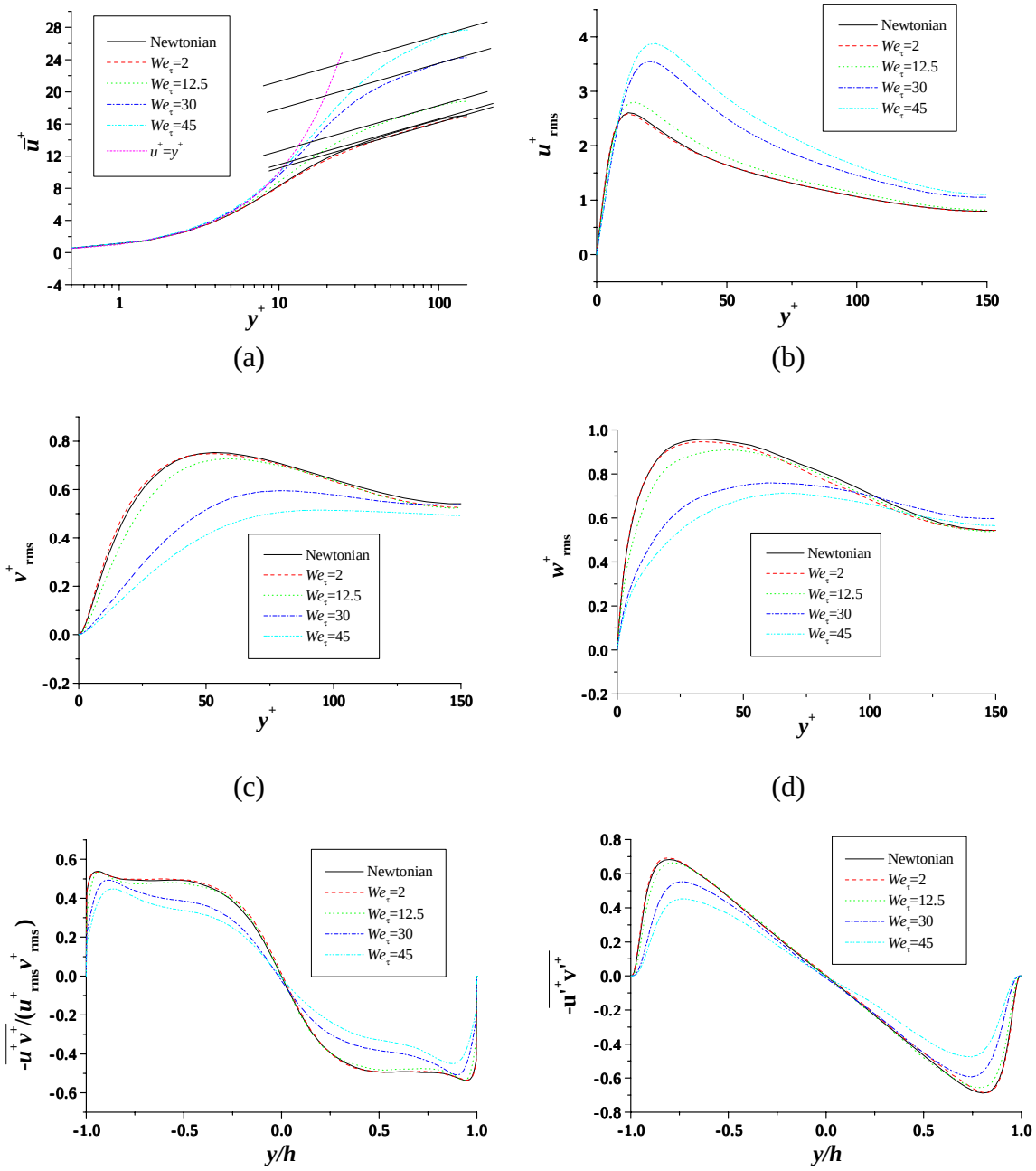

Figure 3: Statistical steady values for Newtonian fluid flow at $\mathrm{Re}_\tau = 150$ and Giesekus fluid flow at $\beta = 0.9, \mathrm{Re}_\tau = 150, \alpha = 0.001$ and four Weissenberg numbers $\mathrm{We}_\tau = 2, 12.5, 30$ and 45. (a) mean velocity profile; (b)-(d) root mean velocity fluctuations; (e) correlation coefficient of u'^+ and v'^+; (f) Reynolds shear stress.

Weissenberg number. The root mean square velocity fluctuations in the normal direction decrease with the increase of Weissenberg number. On the whole the root mean square velocity fluctuations in the spanwise direction also decrease with the increase of Weissenberg number except that at the center part of the channel, they are enhanced for $\mathrm{We}_\tau = 30$ and 45 cases. We can see that the appreciable enhancement of u^+_{rms} and the depression of v^+_{rms} and w^+_{rms} are located at the buffer layers, while in the corresponding logarithmic layers, the turbulent intensities do not change very much. This clearly shows that the polymer/ surfactant additives affects primarily to the phenomena occurring in the buffer layer.
Figure 3(e) compares the velocity correlation coefficients for u and v. It is seen that with the increase of Weissenberg number the correlation coefficients decrease. The location of the maximum correlation coefficient shifts to the bulk flow as compare to the Newtonian case and viscoelastic non-drag-reduction case $\mathrm{We}_\tau = 2$. Figure 3 (f) compares the Reynolds shear stress profiles. It is seen that the larger the drag-reduction rate is, the smaller the Reynolds shear stress becomes. The location where maximum Reynolds shear stress attains also shifts to the bulk flow for drag-reduction cases as compared to Newtonian results.

Figure 4 shows the instantaneous contour maps of the conformation stress c_{xx} in the middle vertical *x-y* plane of the channel. It is seen that with the increase of Weissenberg number, the conformation stress value increases greatly. The stress gradients near the wall become larger and larger. From this picture, we can partly explain why with the increase of Weissenberg number, the calculation becomes easy to break down. The steep stress gradient is difficult to be captured. Using high-order schemes (for finite difference scheme) or spectral method, the steep gradient cannot be accurately captured and negative conformation stress values can be predicted. The unphysical values changes the flow dynamics and usually result in the breakdowns of the solution. To prevent the numerical breakdown, artificial diffusion methods both for spectral method and finite difference scheme were used by Sureshkumar et al.(1997) and Dimitropoulos et al. (1998), and Min et al. (2001) respectively. The calculation did not break down till $We_\tau = 50$ for the Giesekus fluid by using the artificial diffusion spectral method. However too large artificial diffusion may greatly flatten the steep stress gradient (Yu et al. 2002) and the solution accuracy deteriorates. So the high-resolution schemes such as MINMOD, which have been demonstrated to have a good capability to capture steep gradients, appear unavoidable choice for the realistic simulation of the turbulent viscoelastic flow.

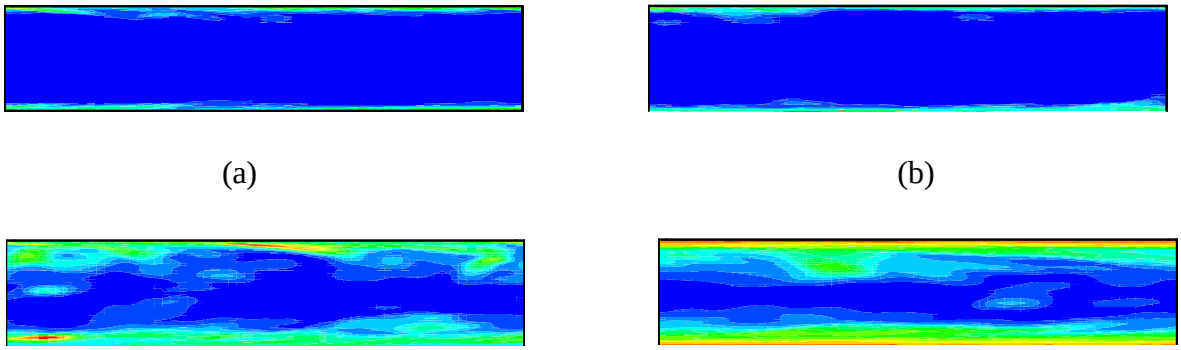

(a) (b)

(c) (d)

Figure 4: Contours of instantaneous C_{xx} in the middle vertical *x-y* plane of the channel for the Giesekus fluid flow at $\beta = 0.9, \mathrm{Re}_\tau = 150, \alpha = 0.001$ and four Weissenberg numbers. (a) $We_\tau = 2$; (b) $We_\tau = 12.5$; (c) $We_\tau = 30$; (d) $We_\tau = 45$. Contour levels for $\mathrm{We}_\tau = 2, 12.5, 30$ and 45 are 1.5-11, 37-545, 68-857 and 107-1520 respectively.

Figure 5 compares the root mean square of C_{xx} fluctuations. It is seen that the conformation stress fluctuations become much stronger with the increase of the Weissenberg number. We believe the strong fluctuations at high Weissenberg number may be another factor to cause the numerical instability and our calculation broke down for a even higher Weissenberg number $We_\tau = 60$ case.

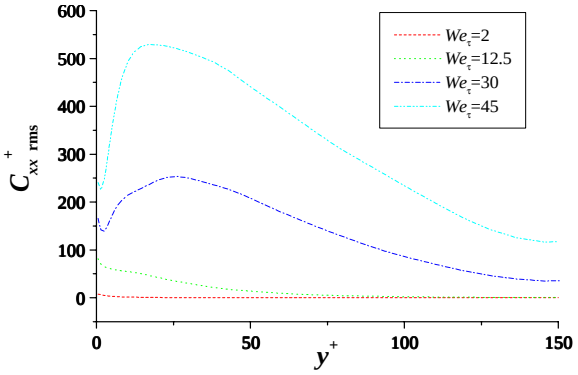

Figure 5: Root mean square fluctuations for conformation stress C^+_{xx} for the Giesekus fluid flow at $\beta = 0.9, \mathrm{Re}_\tau = 150, \alpha = 0.001$ and four Weissenberg numbers $\mathrm{We}_\tau = 2, 12.5, 30$ and 45.

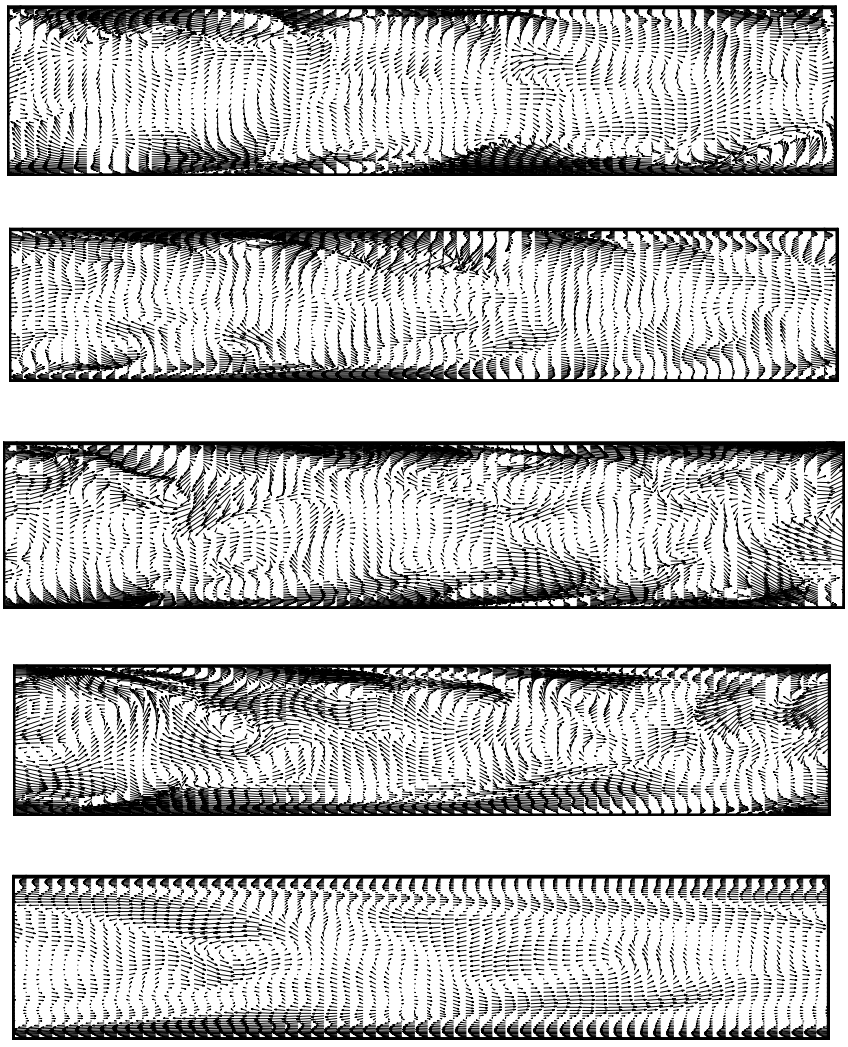

(a)

(b)

(c)

(d)

(e)

Figure 6: Instantaneous velocity fluctuation field in the middle vertical *x-y* plane of the channel for (a) Newtonian fluid flow at $\mathrm{Re}_\tau = 150$ and Giesekus fluid flow at $\beta = 0.9, \mathrm{Re}_\tau = 150, \alpha = 0.001$ and four Weissenberg numbers: (b) $We_\tau = 2$; (c) $We_\tau = 12.5$; (d) $We_\tau = 30$; (e) $We_\tau = 45$

Figure 6 shows the instantaneous snapshots of the velocity fluctuations fields in the middle vertical *x-y* plane of the channel at different Weissenberg numbers (the streamwise velocity components are subtracted by local mean velocity $u^+(y)$). For comparison, an instantaneous velocity field for Newtonian case is also presented. It is clearly seen that the flow structure for no drag-reduction case ($We_\tau = 2$) is similar as that of Newtonian case. With the increase of the Weissenberg number the vortex structure becomes larger, especially in the region near the walls.

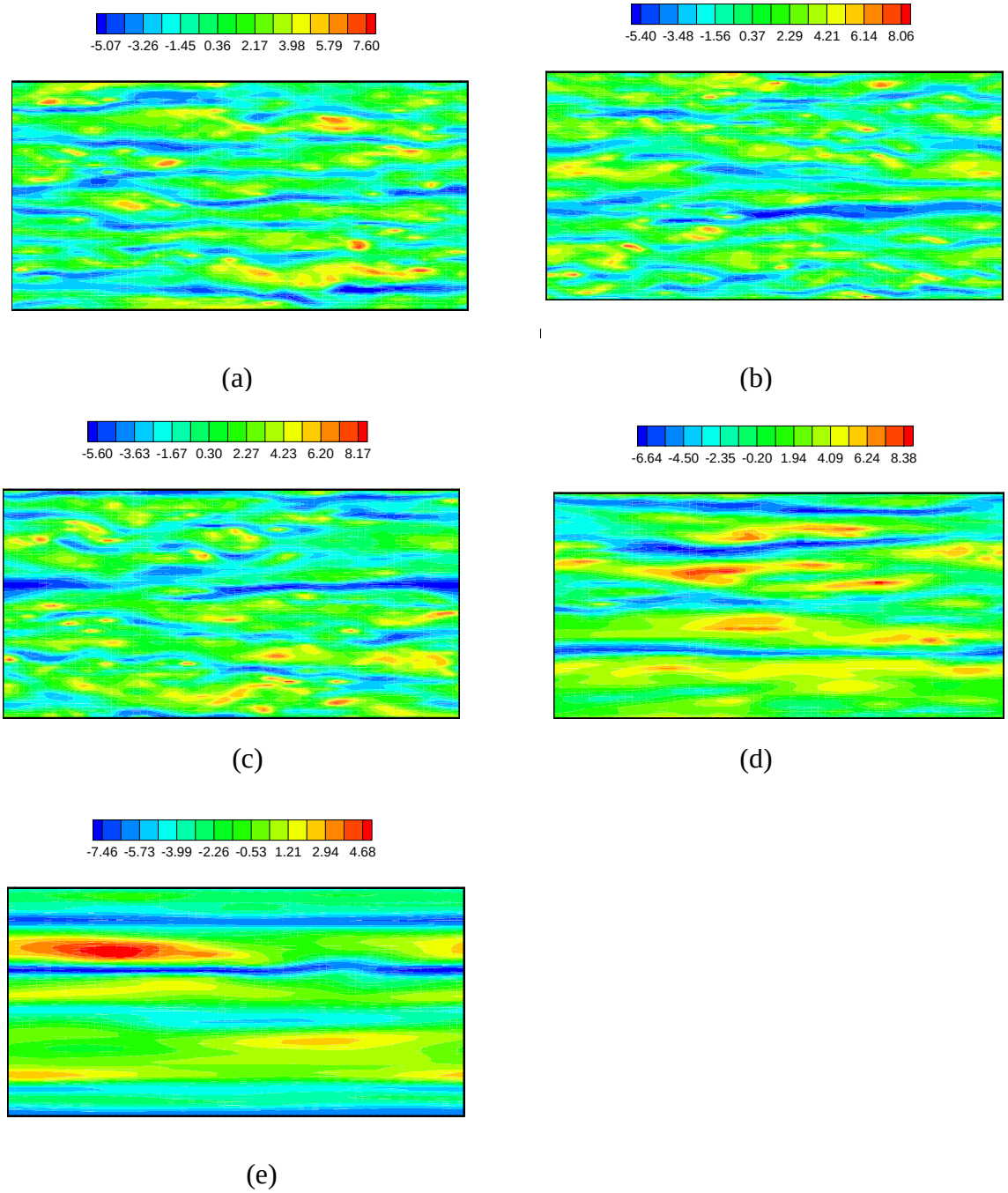

Figure 7: Instantaneous snapshot of streamwise velocity fluctuation in the *x-z* plane at $y^+ = 15$ for (a) Newtonian fluid flow at $\mathrm{Re}_\tau = 150$ and Giesekus fluid flow at $\beta = 0.9, \mathrm{Re}_\tau = 150, \alpha = 0.001$ and four Weissenberg numbers: (b) $We_\tau = 2$; (c) $We_\tau = 12.5$; (d) $We_\tau = 30$; (e) $We_\tau = 45$.

In Figure 6 (e), at the region near the bottom wall, the fluid flows from the right to the left. That means there exist elongated low speed streamwise streaks. To solve the larger flow structure, larger computational domain may require. The effect of computational domain size on the solutions is now carrying out in our research group.

Figure 7 shows the instantaneous snapshots of the streamwise fluctuating velocity in the *x*-*z* plane at $y^+ = 15$. It is seen that with the increase of Weissenberg number, the low speed streaks become more elongated and the average spacing of the streaks become wider. The larger spacing is connected with larger flow structure such as that shown in Figure 6. Figure 8 shows the two-point correlations of streamwise velocity R_{uu} in the spanwise direction. The separation at which the minimum R_{uu} occurs can be used to estimate the mean spacing between high- and low-speed streaks, that is, the mean streak sapcing is roughly twice of the distance to the negative peak. It is seen more clearly from this picture that with the increase of Weissenberg number the streak spacing becomes larger.

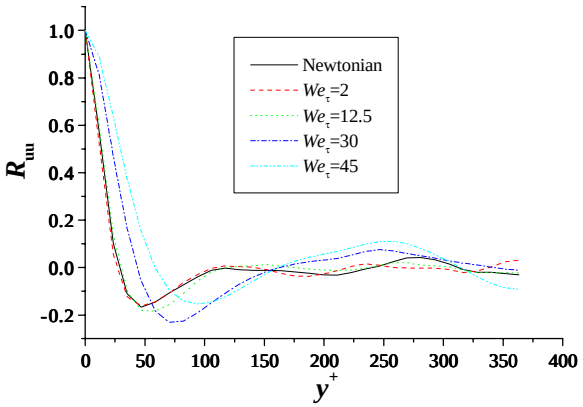

Figure 8: Two-point spanwise correlation of the velocity component in the streamwise direction at $y^+ = 15$ for Newtonian fluid flow at $\mathrm{Re}_\tau = 150$ and Giesekus fluid flow at $\beta = 0.9, \mathrm{Re}_\tau = 150, \alpha = 0.001$ and four Weissenberg numbers $\mathrm{We}_\tau = 2,\ 12.5,\ 30$ and 45.

CONCLUSION

MINMOD scheme is used for the DNS study of Giesekus fluid in a 2D channel. What we concern is the effect of elasticity on the flow structure. Thus in this study we change the Weissenberg number We_τ from 2 to 45 with fixed other parameters $\beta = 0.9, \mathrm{Re}_\tau = 150$ and $\alpha = 0.001$. From the numerical simulations, following conclusions can be drawn. With the increase of Weissenberg number the flow structures become larger. The larger the drag-reduction rate is, larger the u^+_{rms} increases and the smaller the v^+_{rms} and w^+_{rms} decrease. The Reynolds shear stress becomes smaller with the increase of Weissenberg number. The larger the Weissenberg number, the larger the streak spacing become and the larger the drag-reduction is. The onset Weissenberg number obtained in the present study is around 10. The maximum drag-reduction obtained in the present study is 53%.

REFERENCE

Dean R.B. (1978). Reynolds Number Dependence of Skin Friction and Other Bulk Flow Variables in Two-dimensional Rectangular Duct Flow. *Trans. ASME, Journal of Fluids Engineering*100, 215-223.

DenToonder J.M.J., Hulsen M.A., Kuiken G.D.C. and Nieuwstadt F.T.M. (1997). Drag Reduction by Polymer Additives in a Turbulent Pipe Flow: Numerical and Laboratory Experiments. *J. Fluid Mechanics* 337, 193-231.

Dimitropoulos C.D., Sureshkumar R. and Beris A.N. (1998). Direct Numerical Simulation of Viscoelastic Turbulent Channel Flow Exhibiting Drag Reduction: Effect of the Variation of Rheological Parameters. *J. Non-Newtonian Fluid Mechanics* 79, 433-468.

Li P.W., Kawaguchi Y. and Yabe A. (2001). Transient Heat Transfer and Turbulent Characteristics of Drag-reducing Flow Through a Contracted Channel. *Enhanced Heat Transfer* 8, 23-40.

Min T., Yoo J.Y., Choi H. and Joseph D.D.(2001). A Role of Elastic Energy in Turbulent Drag Reduction by Polymer Additives. *Turbulence and Shear Flow Phenomena*, Second International Symposium, KTH, Stockholm, 3, 35-50.

Orlandi P. (1995). A Tentative Approach to the Direct Simulation of Drag Reduction by Polymers, *J. Non-Newtonian Fluid Mechanics* 60, 277-301.

Sureshkumar R., Beris A.N. and Handler R. A. (1997). Direct Numerical Simulation of Turbulent Channel Flow of a Polymer Solution. *Phys. Fluids* 9, 743-755.

Toms B.A. (1948). Some Observations on the Flow of Linear Polymer Solutions Through Straight Tubes at Large Reynolds Numbers, *Proc. 1st Int. Congress on Rheology, II,* 135-141, North Holland, Amsterdam

Yu B. and Kawaguchi Y. (2002), The DNS Study of the Drag-Reducing Viscoelastic Flow With Two Different Spatial Discretization Schemes for the Stress Derivatives, Submitted to *the* S*econd International Conference on Computational Fluid Dynamics*, Sydney.